学位論文（要約）

Study on the role of *interleukin-11* in tail regeneration of *Xenopus laevis* tadpoles

（アフリカツメガエル幼生の尾再生において
インターロイキン 11 が果たす役割に関する研究）

平成 28 年 12 月　博士(理学)申請

東京大学大学院理学系研究科

生物科学専攻

辻岡　洋

Abstract

The ability to regenerate lost organs varies depending on the animal species and the developmental stage. *Xenopus laevis* tadpoles possess remarkable tail regenerative ability, and they are thus used as model animals for studying the molecular mechanisms of organ regeneration. In the regeneration of an organ such as the tail, various tissues are reconstructed to form an ordered structure of the whole organ. Therefore, the origin of various tissues that constitute the organ and the mechanisms by which the organ is coordinately reconstructed are important issues. In *X. laevis* tail regeneration, an earlier study reported that lineage-restricted tissue stem cells are the main source of the regenerated tissues, but the mechanisms of the induction, maintenance, and differentiation of progenitor cells are poorly understood.

In Chapter 1, I hypothesised that undifferentiated cells in the blastema have specific molecular mechanisms that regulate their proliferation and differentiation. To test this hypothesis, I searched for genes selectively expressed in proliferating blastema cells. First, to determine when undifferentiated cells begin to accumulate at the blastema, I performed 5-bromo-2'-deoxyuridine (BrdU) labelling, and found that proliferating cells began to accumulate at the regenerating tail blastema 3 days post-amputation (dpa). Next, to identify regeneration specific molecules, I used RNA-sequencing (RNA-seq) to compare the gene expression profiles of proliferating blastema cells at 3 dpa, which were isolated using a cell sorter based on their DNA content; non-proliferating blastema cells; and proliferating tailbud cells. Quantitative reverse transcription-polymerase chain reaction (qRT-PCR) confirmed that among 36 genes screened for proliferating blastema cell-selective genes, 10 were expressed at significantly higher levels in tail blastema compared to the intact tails and tailbuds. Double-labelling with BrdU labelling and whole mount *in situ* hybridisation (WISH) revealed that

among these 10 genes, at least *interleukin-11* (*il-11*) and *keratin 18* were expressed in the proliferating cells of tail blastema.

以降の内容（第 2 章）に関しては 5 年以内に雑誌等で刊行予定のため、非公開。

Contents

第 2 章に関しては 5 年以内に雑誌等で刊行予定のため、非公開。

Abbreviations

AcGFP, *Aequorea coerulescens* green fluorescent protein

ankrd2, *ankyrin repeat domain 2* (*stretch responsive muscle)*

BrdU, 5-bromo-2'-deoxyuridine

cdk1, *cyclin-dependent kinase 1*

CDS, coding sequence

cse1l*, chromosome segregation 1-like*

CMV, cytomegalovirus

CRISPR/Cas9, clustered regularly interspaced short palindromic repeat/CRISPR-associated 9

dcx, *doublecortin*

DDBJ, DNA Data Bank of Japan

DMSO, dimethyl sulfoxide

dpa, days post amputation

dpf, days post fertilisation

ef1α, *elongation factor 1 alpha*

FACS, fluorescence activated cell sorter

FPKM, Fragments Per Kilobase of exon model per Million mapped fragments

GFP, green fluorescent protein

gRNA, guide RNA

hpa, hours post amputation

il, *interleukin*

IL6ST, IL-6 signal transducer

IL11RA, IL-11 receptor alpha

jak*, janus kinase*

ISH, *in situ* hybridisation

KD, knock down

l1td1*, LINE-1 type transposase domain-containing protein 1*

lrrc2, *leucine rich repeat containing 2*

MEK, Mitogen-activated protein/extracellular signal-regulated kinase kinase

muc5b, *mucin 5, subtype B, tracheobronchial*

not, *notochord homeobox*

oax*, oocyte activation in Xenopus*

pgam2, *phosphoglycerate mutase 2*

phyhd1, *phytanoyl-CoA dioxygenase domain containing 1*

PI3K, Phosphatidylinositol-3 kinase

prkag3, *protein kinase, AMP-activated, gamma 3 non-catalytic subunit*

ptx4, *pentraxin 4*

pygm, *muscle glycogen phosphorylase*

qRT-PCR, quantitative reverse transcription-polymerase chain reaction

RNA-seq, RNA-sequencing

runx1, *Runt-related transcription factor 1*

St., Nieuwkoop and Faber stage

Stat, Signal transducers and activators of transcription

SVL, snout to vent length

tyr*, tyrosinase*

umod, *uromodulin*

UTR, untranslated region

WISH, whole mount *in situ* hybridisation

General Introduction

The ability to regenerate lost organs varies depending on the animal species (Stoick-Cooper et al., 2007). For example, mammals constitutively turn over blood cells, skin, intestinal epithelium, and other tissues. They, however, have poor regenerative abilities for lost organs other than the liver (Miyajima et al., 2014). On the other hand, fish and amphibians have high organ regenerative ability as well as high tissue regenerative ability. Zebrafish can regenerate a fin or heart, and axolotl and newt can regenerate limbs and tails (Stoick-Cooper et al., 2007). Why the regenerative ability, which is advantageous to survive, varies among animal species is an intriguing and important question in basic biology. Clarification of the molecular mechanisms that underlie vertebrate organ regeneration is also important for the advancement of regenerative medicine.

For the regeneration of organs comprised of various tissues, coordinated reconstruction of the tissues is necessary. Therefore, the origin of these tissues and the mechanisms that regulate the proliferation and differentiation of the cells that constitute the tissues are important issues for understanding the mechanism specific to organ regeneration. *Xenopus laevis* tadpoles possess a prominent ability to regenerate amputated tails, which are comprised of various tissues, such as notochord, muscle, and spinal cord (Beck et al., 2009). After tail amputation, a specialised epithelium called wound epithelium covers the amputated plane first. Then the mass of undifferentiated proliferating cells called the blastema appears, and the undifferentiated cells are properly differentiated to form a new tail. Cell lineage tracing revealed that the main source of tail is not dedifferentiated pluripotent stem cells, but rather lineage-restricted tissue stem cells (Gargioli and Slack, 2004). The molecular mechanisms that underlie the induction, maintenance, and differentiation of progenitor cells, however, are not well understood.

In this study, I focused on *il-11*, which showed most remarkable blastema-

selective expression among proliferating blastema cell-selective genes that I identified. IL-11 is a member of the IL-6 family. The IL-6 family transduces signals through the signal transducers and activators of transcription (Stat) 1/3 pathway, mitogen-activated protein/extracellular signal-regulated kinase kinase (MEK) pathway, or phosphatidylinositol-3 kinase (PI3K) pathway (Ernst and Putoczki, 2014) (Fig. 1). *il-11* is expressed in the regenerating heart of zebrafish, and forced expression of a dominant negative form of Stat3 inhibits the proliferation of cardiomyocytes and heart regeneration (Fang et al., 2013). The role of *il-11* in regeneration of organ which is comprised of various tissues is, however, not understand.

以降の内容（第 2 章）に関しては 5 年以内に雑誌等で刊行予定のため、非公開。

Chapter 1

Analysis of the gene expression profile of isolated proliferating blastema cells in regenerating *Xenopus laevis* tadpole tails

Introduction

Organ regenerative ability varies depending on the animal species and developmental stage (Stoick-Cooper et al., 2007). The molecular bases underlying the variable organ regenerative abilities, however, remain largely unknown. Aiming at identifying the genes involved in organ/tissue regeneration, extensive studies have been performed using various animals with high organ regenerative ability (Lin et al., 2013; Liu et al., 2013; Love et al., 2013; Sikes and Newmark, 2013; Umesono et al., 2013; Whitehead et al., 2005). Recent studies have performed transcriptomic analyses of the regenerating tissues of amputated organ stumps, using frog/tadpole tails or limbs or axolotl limbs (Grow et al., 2006; Knapp et al., 2013; Love et al., 2011; Monaghan et al., 2009; Pearl et al., 2008; Tazaki et al., 2005; Wu et al., 2013b). These studies, however, do not completely elucidate the underlying organ regeneration processes.

In contrast to variable regenerative ability, all animals undergo organogenesis during normal developmental process, and thus there should be specific factors or mechanism to enable regeneration other than normal development. One of the obstacles that has impeded the progress of organ regeneration research is the difficulty in distinguishing factors specific to organ regeneration and factors commonly involved in both regeneration and organogenesis. Many factors are likely involved in both organ regeneration and organogenesis. Therefore, I planned to identify regeneration specific molecules which would be important for elucidating organ regeneration processes.

To reveal regeneration specific mechanisms, I focused on the proliferating blastema cells in regenerating *Xenopus laevis* tadpole tails. *X. laevis* tadpoles possess high tail regenerative ability except during the ‘refractory period’ when this ability is transiently lost (Beck et al., 2003). Fukazawa et al. (2009) previously used the differential display method to comprehensively search for genes whose expression differs in amputated tadpole tail stumps between the ‘refractory period’ and the

subsequent ‘post-refractory regeneration period’. Fukazawa et al. found that distinct immune responses occur in the amputated tadpole tail stumps between these two periods, and that immunosuppressant treatment drastically restores regenerative ability during the refractory period. Various immune-related genes such as *T Cell Receptor*, a T cell marker, begin to be expressed in the whole tadpole body at the onset of the refractory period, whereas the expression of *forkhead box P3*, a regulatory T cell marker, is more enriched in the amputated tail stumps in the post-refractory regeneration period than in the refractory period. Based on these findings, Fukazawa et al. proposed that autoreactive immune cells attack blastema cells as ‘non-self’, which results in impaired tail regenerative ability during the refractory period, whereas regulatory T cells suppress autoreactive immune cells, which enables regeneration during the post-refractory regeneration period (Fukazawa et al., 2009). The postulated ‘autoantigen(s)’ might be expressed in proliferating cells of blastema.

In Chapter 1, I aimed to clarify the gene expression profile specific to proliferating *X. laevis* tadpole tail blastema cells to identify candidate genes involved in the tail regeneration and possible ‘autoantigen(s)’ by identifying genes that are selectively expressed in proliferating blastema cells compared to non-proliferating blastema cells or proliferating cells of developing tailbuds.

Results

Isolation of proliferating tadpole tail blastema cells

First, I intended to isolate proliferating tadpole tail blastema cells to identify genes selectively expressed in proliferating blastema cells. To collect enough amount of cells for transcriptomic analysis, I examined when proliferating cells appear in blastema. I used post-refractory regeneration period tadpoles (Nieuwkoop and Faber stage (Nieuwkoop and Faber, 1994) (St.) 49-53, the stage did not proceed during the experiments at least morphologically), because larger body size of them will be advantageous to collect blastema cells compared to pre-refractory regeneration period tadpoles. I labelled 5-bromo-2'-deoxyuridine (BrdU) positive cells of tail stumps of tadpoles at 1, 2, 3, and 4 days post amputation (dpa). It revealed that the BrdU-positive cells were enriched in the tail blastema 3 dpa or later (Fig. 2). The expression of regeneration specific genes might decline in very late phases of regeneration. Therefore, I determined to collect the earliest enriched proliferating cells from 3-dpa blastemas. Next, I intended to identify genes specific to regeneration and not used in tail development. For this, I intended to collect proliferating tailbud cells from tailbud stage embryos as a control. BrdU labelling of tailbuds of the St. 35-39 tailbud stage embryos detected many BrdU-positive cells in the tailbud (Fig. 3). Then I tried to isolate the proliferating cells from these blastemas and tailbuds for transcriptomic analysis.

To perform transcriptomic analysis of the proliferating tail blastema cells, it was necessary to collect living cells. BrdU labelling cannot be used for this purpose, because the BrdU-labelled cells need to be fixed when BrdU is detected, which severely impair the recovery of transctipts. Therefore, I used fluorescence activated cell sorter (FACS) to collect the cell fraction whose DNA content was $4x$ ($S/G_2/M$ phases) using Hoechst 33342, which is a nucleic acid stain permeable to live cell membrane. Single cell suspensions of the tail blastema and tailbuds were prepared and stained with

Hoechst 33342 for DNA staining, and propidium iodide for dead cell staining (Fig. 4). When these cells were subjected to FACS for cell cycle analysis, in both the tail blastema and tailbud, a major peak appeared that corresponded to G_0/G_1 phases. A cell population whose DNA contents were larger than those of the cells in the major peak and equal to or smaller than twice of those of the cells in the major peak also appeared, and seemed to correspond to $S/G_2/M$ phases (Fig. 5). I isolated the cell fraction that corresponds to the $S/G_2/M$ phases (hereafter referred to as '4*x*-tail blastema' cell fraction or R4 (regenerating 4*x* cell fraction)) for the tail blastema. I also isolated the cell fraction that corresponds to the G_0/G_1 phases (hereafter referred to as '2*x*-tail blastema' cell fraction or R2) from the tail blastema sample as the non-proliferating tail blastema cells as a control, as well as the cell fraction that corresponds to the $S/G_2/M$ phases (hereafter referred to as '4*x*-tailbud' cell fraction or E4 (embryonic 4*x* cell fraction)) from the tailbud sample as the proliferating tailbud cells as another control. As very large amounts of samples (1 μg of total RNA, approximately 1×10^5 cells) were needed for the RNA-sequencing (RNA-seq) analysis, FACS was performed repeatedly and several batches of cell fractions were combined into single cell fractions. Figs. 5a and b are representative images of each FACS experiment. During the cytometry experiment, fluorescent intensity of the cells slightly and continuously changed. Therefore, the gating criteria for the R4 and R2, and E4 and E2, could not be determined strictly throughout the experiments, and slightly varied depending on the individual experiment. However, the later expression analysis of cell cycle marker genes indicated that proliferating cells and non-proliferating cells were separated successfully by this gating criteria (see Fig. 6).

RNA-seq analysis of proliferating blastema cells, non-proliferating blastema cells, and proliferating tailbud cells

The RNAs extracted from proliferating blastema cell, non-proliferating blastema cell, and proliferating

tailbud cell fractions were then subjected to RNA-seq analysis. To identify genes specific to regeneration, non-proliferating blastema cells were used as a negative control cells to exclude genes which are not related to regeneration-specific cell proliferation, and proliferating tailbud cells were used as another negative control cells to exclude genes expressed in the developing tail. Approximately 80 million paired-end reads of length 100 bp for each sample were sequenced. The data was deposited in the DNA Data Bank of Japan (DDBJ, Accession No. DRP002318). The sequenced reads were then mapped onto the *X. laevis* draft genome 7.0 (James-Zorn et al., 2013; Langmead et al., 2009; Trapnell et al., 2012). The new gene models were generated using Cufflinks (Trapnell et al., 2012) with a help of reference model, XlaevisJGIv1.3.primaryTrs.gff3, and gene expression levels were estimated using Cufflinks (Trapnell et al., 2012). The overall alignment rate was approximately 70%, and approximately 60% reads were aligned uniquely, which indicated that most reads were mapped onto collect genes, even though *X. laevis* is known as allotetraploid.

The gene expression levels of *cyclin-dependent kinase 1 (cdk1)* (McGowan et al., 1990) and *cyclin B2* (Wasner et al., 2003), both of which are cell cycle markers for G_2/M phase cells in vertebrates, were approximately 20-folds higher in both R4 and E4 cell fractions than in the R2 cell fraction (Fig. 6), confirming that the cells in the G_2/M phases are enriched in the R4 and E4 cell fractions.

The number of genes whose fragments per kilobase of exon model per million mapped fragments (FPKMs) were up-regulated more than 2-fold in R4 than in R2 was smaller than that in R4 than in E4 (Fig. 7a). Similarly, the number of genes that were down-regulated for more than 2-fold in R4 than in R2 was smaller than that in R4 than in E4 (Fig. 7b). These observations suggest that the expression pattern between R4 and R2 is more similar than that between R4 and E4.

Identification of genes expressed preferentially in proliferating tail blastema cells

As candidate genes expressed preferentially in the proliferating tail blastema cells, I identified the

genes whose expression levels were more than two times higher in the R4 cell fraction than in the R2 and E4 cell fractions. Because biological or technical perturbation affect the estimation of gene expression more severely in genes with low expression than in genes with high expression, the estimation of fold change of genes with low expression is inaccurate. Therefore I excluded genes with low expression by selecting genes whose FPKMs for the R4 cell fraction exceeded 1, which corresponds to approximately 1/1000 of that of *elongation factor 1 alpha* (*ef1α*) (Fig. 7c). However, considering the lack of replication of RNA-seq data, which limits the accuracy of the estimation of gene expressions, I decided to use a more stringent cutoff, FPKM > 10 (Fig. 7d). As a result, 412 genes were listed as candidate genes. I found that only a few reads were mapped onto some candidate genes in very short (~100 bp) unassembled scaffolds. Assuming that estimations of FPKM from only a few mapped reads were inaccurate, I chose 70 genes, whose maximum depth of uniquely mapped reads was at least 50. I also excluded genes whose FPKM or gene models were considered to be inaccurate (for example, some short gene models were found in a narrow region of a scaffold, and many reads were mapped not only on the genes, but also on the regions between the genes, indicating that the genes are not different genes, but actually different regions of one gene), and finally selected 41 genes. After exclusion of contaminated ribosomal RNA genes, a total of 36 genes were listed as candidates (Fig. 7e).

To confirm the reproducibility of differential gene expression of candidate genes identified by RNA-seq analysis, I performed quantitative reverse transcription-polymerase chain reaction (qRT-PCR). As the expression levels of some candidate genes might have been perturbed during the cell dissociation and isolation procedures, I examined the expression levels of the candidate genes at the organ/tissue level using tail blastemas, intact tail tissues, and tailbuds. Among the 36 candidate genes, I could design appropriate primers for qRT-PCR in 28 genes. 10 genes (*interleukin-11* (*il-11*), *keratin 18, brevican, chromosome segregation 1-like* (*cse1l*), *lysyl oxidase, LINE-1 type transposase domain-*

containing protein 1-like (*l1td1-like*), *cd200like-related, oocyte activation in Xenopus* (*oax*), and two uncharacterized genes) of the 28 genes were expressed at significantly higher levels in the tail blastemas than in the intact tail tissues and tailbuds (Fig. 8). Some of their expression levels in blastema were upregulated less than 2-fold compared to intact tail or tailbud, although selection criteria for them in RNA-seq analysis was more than 2-fold upregulation in R4 than in R2 and E4. It is possible that expression levels of them were altered during cell dissociation and cell sorting procedures.

I annotated these genes based on the homology search using blast (Altschul et al., 1990) (Table 1). The complete coding sequence (CDS) of *il-11*, which showed most striking blastema-selective expression, was experimentally determined (DDBJ, Accession No. AB933563). I also tried to identify longer sequences of the gene fragments of *l1td11-like, cd200like-related,* and *uncharacterized gene 2*, which were too short for designing appropriate probes for whole mount *in situ* hybridisation (WISH), by 3' rapid amplification of a cDNA end and de novo assembly using the sequenced reads (DDBJ, Accession No. DRP002318), and obtained the complete CDS of *cd200like-related* (DDBJ, Accession No. AB933564), and the partial CDS of *l1td1-like* (DDBJ, Accession No. AB933565).

I next used WISH to examine the location where the candidate genes are expressed in the tail blastema. Among the 10 genes, I could design appropriate probes and performed WISH for 8 genes, *il-11*, *cse1l*, *keratin 18*, *brevican, lysyl oxidase, l1td1-like, cd200like-related,* and *uncharacterised gene 1*. Among them, I detected WISH signals for 5 genes, *il-11, cse1l, keratin 18, brevican,* and *lysyl oxidase* (Fig. 9). Because the expression levels of *l1td1-like, cd200like-related,* and *uncharacterised gene 1* were lower than the 5 genes, their expression levels might be below the detection threshold. All five genes were expressed preferentially in the tail blastema, but their expression patterns in the tail blastema differed slightly. Both *il-11* and *cse1l* were expressed in the broad region of the tail blastema, whereas *keratin 18, brevican,* and *lysyl oxidase* were expressed mainly in the notochord bud

(tip of the regenerating notochord). Both *keratin 18* and *brevican* were also weakly expressed in the spinal cord ampulla (tip of the regenerating spinal cord), and *keratin 18* was also very weakly expressed in the round cells at the surface of the blastema, which might be wound epithelium.

Finally, to identify the cell populations expressing these five genes in the proliferating tail blastema cells more precisely, I performed double-labelling of BrdU-labelling and WISH for the five genes. The WISH signals of *il-11* and *keratin 18* were detected in restricted cell populations located at the inner regions of the BrdU-positive tail blastema cells (Fig. 10).

Discussion

In the present study, I analysed gene expression profiles of *X. laevis* proliferating tail blastema cells, non-proliferating tail blastema cells, and proliferating tailbud cells using FACS. It is important to note that the non-proliferating cell population may include some proliferating G_1 cells, which might obscure the difference between the proliferating cells and non-proliferating cells, and some proliferating blastema cell-selective genes might be overlooked. Some genes selectively expressed in proliferating blastema cells might have been perturbed during the cell dissociation and cell sorting procedures, and were also not selected as proliferating blastema cell-selective genes in RNA-seq analysis. Therefore, it is possible that some other genes involved in tail regeneration could be identified in the future research.

I performed a comprehensive search for genes expressed preferentially in the proliferating tail blastema cells in *X. laevis* tadpoles to identify 10 genes, *il-11*, *keratin 18*, *brevican*, *cse1l*, *lysyl oxidase*, *l1td1-like*, *cd200like-related*, *oax*, and two uncharacterised genes (Fig. 8). Among them, *il-11* and *cse1l* were expressed in a broad area of the tail blastema, whereas *brevican*, *lysyl oxidase*, and *keratin 18* were mainly expressed in notochord buds (Fig. 9). The finding that three of the five identified genes were expressed preferentially in the notochord bud likely reflects the relatively high ratio of notochord bud cells in the proliferating tail blastema cells (Fig. 2c).

Among the genes whose preferential expression in tail blastema was confirmed by qRT-PCR, L1td1 is an RNA-binding protein required for self-renewal of human embryonic stem cells and proliferation of cancer cells (Närvä et al., 2012). It is thus possible that *l1td1-like* is required for self-renewal of proliferating tail blastema cells, even in *X. laevis* tadpoles. Localisation of the expression of *l1td1-like*, however, was not analysed in this study. Analysis of the localisation of the expression of *l1td1-like*, and other genes whose signals were not detected in this study, will be important in the future

studies.

cd200 encodes an immunoglobulin superfamily membrane glycoprotein, which suppresses overactivation of the immune system in mice (Hoek et al., 2000). A CD200 isoform antagonises CD200 to inhibit its immunosuppressive action (Chen et al., 2008). It is thus possible that *cd200like-related* plays a role in the modulation of autoimmune responses to tail blastema cells during the refractory period.

oax is a repetitive element transcribed by somatic nuclei when injected into the nuclei of *X. laevis* oocytes (Wakefield et al., 1983) and is thought to have originated by tandem duplication of a short interspersed repetitive element (Okada, 1991). A transcript of a short interspersed repetitive element of mouse, B2 RNA, associates with RNA polymerase II to repress the transcription of certain genes during heat shock responses (Allen et al., 2004). Interestingly, *oax* is expressed in the amputated stumps of regenerating *X. laevis* tadpole limbs (King et al., 2003). Therefore, it is possible that *oax* plays a role in regulating gene expression in the tail blastemas, although the function of *oax* has not been clarified.

Among the five genes whose preferential expression in the tail blastema was confirmed by WISH, *cse1l* is highly expressed in proliferating cells (Wellmann et al., 1997), and its reduction leads to an accumulation of G_2-arrested cells (Ogryzko et al., 1997) in mammals. It is thus plausible that *cse1l* plays a role in regulating the cell cycle of proliferating tail blastema cells in the regenerating *X. laevis* tadpole tails.

Previous studies reported that *brevican* (Sander et al., 2001) and *lysyl oxidase* (Geach and Dale, 2005) are expressed in the notochord of the *X. laevis* embryos. *brevican* encodes a member of aggrecan-versican family proteoglycans that constitutes a component of the extracellular matrix (Frischknecht and Seidenbecher, 2012). *lysyl oxidase* catalyses the covalent crosslinking of the side chains of amino acid residues of collagen and elastin to stabilise the extracellular matrix (Nishioka et

al., 2012). *X. laevis* embryos treated with β–aminoproprionitrile, a specific inhibitor of the catalytic activity of Lysyl oxidase family enzymes, develop kinks in the notochord (Geach and Dale, 2005). It is thus highly likely that *brevican* and *lysyl oxidase* comprise the extracellular matrix, not only in the notochord during tail development but also in the notochord bud during tail regeneration.

In Chapter 1, I demonstrated that *il-11* and *keratin 18* are actually expressed in a restricted cell population of proliferating tail blastema cells. The signals for the other genes were not detected. To detect the signals for the other genes, it will be important to design other probes targeting different regions of the genes, or performing immunohistochemistry using antibodies against the product of these genes. Examining whether these genes were expressed in proliferating blastema cells will be important for further analyses of these genes.

A previous study reported that *keratin 18* is expressed in the regenerating newt limb blastema, and is necessary for cell proliferation (Corcoran and Ferretti, 1997). Therefore, it is likely that *keratin 18* is also involved in the proliferation of notochord bud cells in the regenerating *X. laevis* tadpole tails.

It is possible that *il-11* expression in the proliferating tail blastema cells represents an immune response upon tail amputation. Viral (Bartz et al., 2002) and bacterial (Kernacki et al., 1998) infection or stimulation by cytokines such as Interleukin-1, Tumor Necrosis Factor-α, and Transforming Growth Factor-β1 induce *il-11* expression in mammalian dendritic cells, macrophages, and other tissues (Bamba et al., 2003). IL-11 stimulates megakaryocytopoiesis in human bone marrow mononuclear cells (Teramura et al., 1992), which results in increased platelet production, and to inhibit the production of proinflammatory cytokines from lipopolysaccharide-stimulated macrophages (Trepicchio et al., 1996). Thus, it might be that IL-11 produced by the proliferating tail blastema cells facilitates wound healing and creates the appropriate conditions for successful tail regeneration in *X. laevis* tadpoles. On the other hand, a recent work reported that *il-11* is highly expressed in the injured

heart of zebrafish, and its downstream signalling molecule, *janus kinase 1 (jak1)/signal transducers and activators of transcription 3 (stat3)* is required for heart regeneration (Fang et al., 2013). Therefore, regenerating tadpole tail may also need *jak1/stat3* signalling activated by *il-11*. In addition, another study recently suggested that IL-11 contributes to maintain the pluripotent state in human embryonic stem cells (Peterson et al., 2013). It is thus also plausible that *il-11* contributes to maintain the pluripotent state of proliferating tail blastema cells in *X. laevis* tadpoles. Gargioli and Slack (2004) reported that tissue-specific stem cells restricted to their cell lineages, but not dedifferentiated pluripotent stem cells, contribute to regenerate tissues in the *X. laevis* tadpole tail regeneration (Gargioli and Slack, 2004). Expression of *il-11* in a broad area of the tail blastema, except the wound epithelium, suggests that *il-11* is involved in molecular mechanism(s) that are rather common among various cell lineages in the tail blastema of *X. laevis* tadpoles.

To clarify the role of these genes in tail regeneration, functional analysis is necessary. Among these genes, I focued on *il-11* which showed most prominent blastema-selective expression. In Chapter 2, I analysed the role of *il-11* in tail regeneration.

第 2 章の内容に関しては 5 年以内に雑誌等で刊行予定のため、非公開。

Conclusion and Future Perspectives

この内容に関しては 5 年以内に雑誌等で刊行予定のため、非公開。

Materials and Methods

Statistical tests were not used to pre-determine sample size. The experiments were not randomised or blinded. Normally developed tadpoles were used in the experiments.

Animals

Animals were treated essentially as described previously (Naora et al., 2013). Nieuwkoop and Faber stage (Nieuwkoop and Faber, 1994) (St.) 49-53 tadpoles were purchased from a Japanese company (Watanabe Zoushoku), and used as post-refractory period tadpoles. Other tadpoles were obtained by mating wild-type outbred *Xenopus laevis* adults or by artificial fertilisation, and maintaining their offspring in the laboratory. St. 35-39 tailbud stage tadpoles were used for analyses using tailbud in Chapter 1.

この内容に関しては 5 年以内に雑誌等で刊行予定のため、非公開。

All of the surgical manipulations, including the tail amputation, were performed after completely anesthetising the tadpoles with 0.02% MS222 (Sigma-Aldrich, St. Louis, MO) or ice. These experiments were performed in accordance with the recommendations of the Guidelines for Proper Conduct of Animal Experiments of Science Council of Japan. The protocol was approved by the Committee on the Ethics of Animal Experiments of the Graduate School of Science, the University of Tokyo (Permit Number: 19-14 Z 07-08).

BrdU labelling

BrdU labelling was performed essentially as described previously (Isoe et al., 2012). Proliferating cells were labelled with BrdU by exposing the tadpoles to water containing 1 mg/ml BrdU (Sigma-Aldrich)

for 12 h before sampling. Whole bodies (St. 35-39 tadpoles) or tails (St. 49-53 tadpoles) were fixed with Bouin's fixative and embedded in Paraplast (McCormick Scientific, St. Louis, MO). Sections cut 10 μm-thick were prepared and rehydrated, and the antigen was retrieved by 2N HCl treatment for 30 min. Immunohistochemical detection of BrdU was performed using mouse anti-BrdU antibody (BD Pharmingen, San Jose, CA, cat. 555627) and Alexa Fluor 555 goat anti-mouse IgG antibody (Invitrogen, Carlsbad, CA, cat. A-21424), followed by counterstaining with 10 μg/ml Hoechst 33342 (Lonza Cologne GmbH, Germany).

Isolation of proliferating blastema and tailbud embryo cells

Regenerating tail tissues (tail blastemas) were removed with a fine surgical knife from regenerating St. 49-53 tadpole tails 3 days post amputation (dpa). Tailbuds were removed with a fine surgical knife from St. 35-39 tailbud stage embryos. Cell dissociation was performed as described previously (Kragl et al., 2009) with minor modifications. In brief, tissues were incubated in dissociation solution (100 U/ml DNase I (Roche Diagnostics, Indianapolis, IN), 0.25 mg/ml Liberase TM research grade (Roche Diagnostics) in phosphate-buffered saline) at 28°C for 30 min. Cells were then passed through a 30-μm filter and washed.

Isolation of the proliferating cells was performed as described previously (Lin and Goodell, 2006) with minor modifications. In brief, Hoechst 33342 was added to a single cell suspension at a final concentration of 10 μg/ml, the suspension was incubated at 28°C for 30 min, and then washed. Propidium iodide (Molecular Probes, Eugene, OR) was added at a final concentration of 1 μg/ml before cell sorting. The samples were then directly subjected to the cell sorting using FACS Aria (BD Pharmingen).

RNA-seq analysis of isolated cells

Total RNA was extracted from the proliferating tail blastema cells, whose DNA contents were 4*x* (‘4*x*-tail blastema’ cell fraction), non-proliferating tail blastema cells, whose DNA contents were 2*x* (‘2*x*-tail blastema’ cell fraction), and the proliferating tailbud cells, whose DNA contents were 4*x* (‘4*x*-tailbud’ cell fraction) using RNeasy mini kit (Qiagen, Germany). The numbers of cells used were 9.7×10^5 cells (from ~1200 tadpoles) for the ‘4*x*-tail blastema’ cell fraction, 4.0×10^6 cells (from ~1200 tadpoles) for the ‘2*x*-tail blastema’ cell fraction, and 7.6×10^4 cells (from ~150 embryos) for the ‘4*x*-tailbud’ cell fraction. cDNA libraries were generated using TruSeq Stranded Total RNA with Ribo-Zero Gold LT Sample Prep Kit (Illumina, San Diego, CA). I then produced a set of approximately 8.2×10^7 paired end reads (100 bp×2, insert size 160 bp) from each cDNA library using Hiseq 2500 (Illumina). The dataset was deposited in the DNA Data Bank of Japan (DDBJ, Accession No. DRP002318). As very large amounts of samples were needed, it was difficult for me to perform the RNA-seq analysis with multiple replicates. Therefore, I performed RNA-seq with a single set of samples (and thus the statistical analysis was not applicable to this RNA-seq analysis). Rather, I used qRT-PCR to confirm proliferating tail blastema cell-preferential expression of the identified genes with multiple replicates (lots of samples) as described below.

The sequenced reads were mapped to *X. laevis* draft genome 7.0 (LAEVIS_7.repeatMasked.fa) (Xenbase (James-Zorn et al., 2013)) using TopHat (Langmead et al., 2009; Trapnell et al., 2012). To cover the unannotated transcripts, I generated new gene models based on the mapped reads using Cufflinks (Trapnell et al., 2012) with a help of reference model, XlaevisJGIv1.3.primaryTrs.gff3 (Xenbase (James-Zorn et al., 2013)). Expression levels were estimated and compared using Cufflinks and Cuffdiff programs (Trapnell et al., 2012).

qRT-PCR

Expression analysis by qRT-PCR was performed essentially as described previously (Naora et al., 2013) using a LightCycler 1.0 or a LightCycler 480 Real-Time PCR System (Roche Diagnostics, Switzerland). Total RNA was extracted using an RNeasy mini kit (Qiagen) and reverse-transcribed using PrimeScript RT reagent Kit with gDNA Eraser (Perfect Real Time) (TaKaRa, Japan). qRT-PCR was performed using SYBR premix ExTaq II (Tli RNaseH plus) (TaKaRa), and the amount of each transcript was normalised with that of *elongation factor 1 alpha* (*ef1α*), or the amount of total RNA used for reverse transcription. Primers were designed following the manufacture's protocol (TaKaRa). Primers used in qRT-PCR are as follows:

ef1α;

5'-GGAACGGTGACAACATGC-3' and 5'-AGGCAGACGGAGAGGCTTA-3',

il-11;

5'-TCCTGAAGCTAAGCACTGACCT-3' and 5'-TGAATTCCGTTAAATTCGTGGTCCA-3',

keratin 18;

5'- CGCACCATGCAGTCCCTAGA -3' and 5'- ACGTGCTTCTGTGTCGTGGA -3',

brevican;

5'- CAAGTGGGGACGGTTCTGGT -3' and 5'- GGTTGGGTTCCCTGAGTGCT -3',

cse1l;

5'- TCGAGCTTCCCGAAGACGAC -3' and 5'- AGCTGAGAGAAGGCTGCCTG -3',

lysyl oxidase;

5'- CAACAGCAGCGTTTCCCAGG -3' and 5'- GGTTGATGCTCGCAGTCTGC -3',

l1td1-like;

5'- TTGTTGCCGTCCACCACTCG -3' and 5'- AGAGGTCCGGAAGAGGCTCA -3',

cd200like-related;

5’- CCACCTTCTGACTGTGTTGCA -3’ and 5’- TCAGGCAGAGAATGTATTTGCTCT -3’,

uncharacterized gene 1;

5’- GGTTCCACATTGGGCGTCAG -3’ and 5’- GCTAACCCAGCCTCTCAGCT -3’,

oax;

5’- AAAGCACTGCGGACAAGAGC -3’ and 5’- TAGCTCAGTCGGTAGAGCGC -3’,

uncharacterized gene 2;

5’- TGGCACAAGTGTGATGTTTCACG -3’ and 5’- CCCGAACTTTTGTTTCCGTTGTG -3’,

以降の内容に関しては 5 年以内に雑誌等で刊行予定のため、非公開。

cDNA cloning

To determine the putative primary structure of *il-11, l1td1-like,* and *cd200like-related,* I isolated cDNA clones for them. Briefly, total RNA was extracted from 3 dpa tail stumps of St. 49-53 tadpoles using TRIzol (Invitrogen). cDNA was synthesised using SuperScript III First-Strand Synthesis System (Invitrogen) after DNase treatment (DNase I, Invitrogen), or RLM-RCE kit (Life Technologies) for 3’ rapid amplification of a cDNA end as described previously (Fukazawa et al., 2009; Kiya et al., 2008). *De novo* assembly was performed using CLC Genomics Workbench (CLC Bio), following the manufacturer’s protocol. The sequences were deposited in the DDBJ (accession numbers for the nucleotides of *il-11, l1td1-like,* and *cd200like-related* are AB933563, AB933564, AB933565).

WISH

WISH was performed as described previously (Hoppler and Vize, 2012) with minor modifications: 50 μg/ml proteinase K was used, and the samples were incubated overnight for four nights with hybridisation buffer, and bleached with 10% H_2O_2 after the chromogenic reaction.

以降の内容に関しては 5 年以内に雑誌等で刊行予定のため、非公開。

Double-labelling by BrdU-labelling and WISH

BrdU labeling was performed as described above. Double-staining with WISH was performed as described previously (Hoppler and Vize, 2012) with minor modifications in addition to those described above: mRNA was detected using HNPP Fluorescent Detection Set (Roche Diagnostics), and the samples were mounted in scale A2 (Hama et al., 2011), followed by imaging using a confocal microscope.

以降の内容に関しては 5 年以内に雑誌等で刊行予定のため、非公開。

Figures

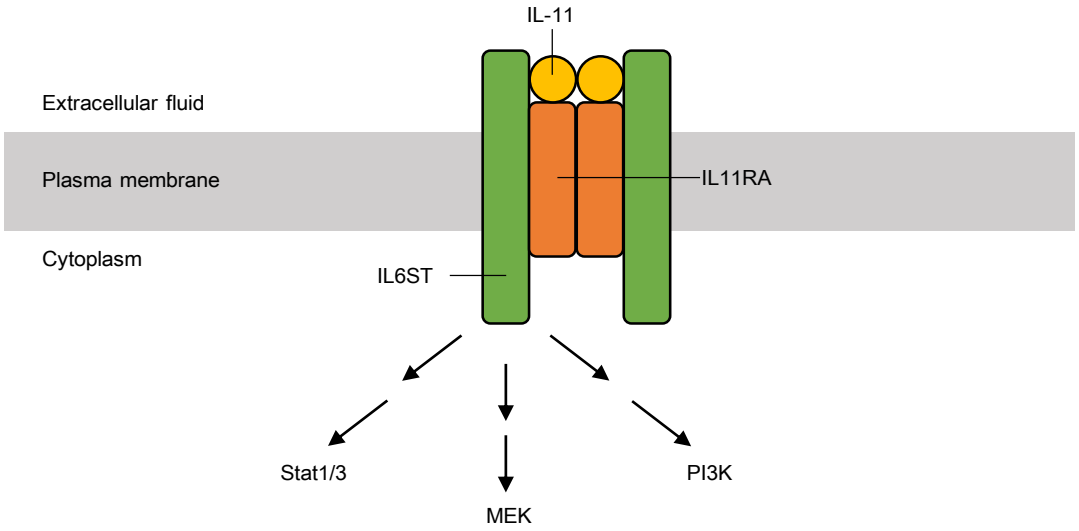

Figure 1 Scheme of the IL-11 signalling pathway

IL11RA is a specific receptor for IL-11, and IL6ST is commonly used among IL-6 family members.

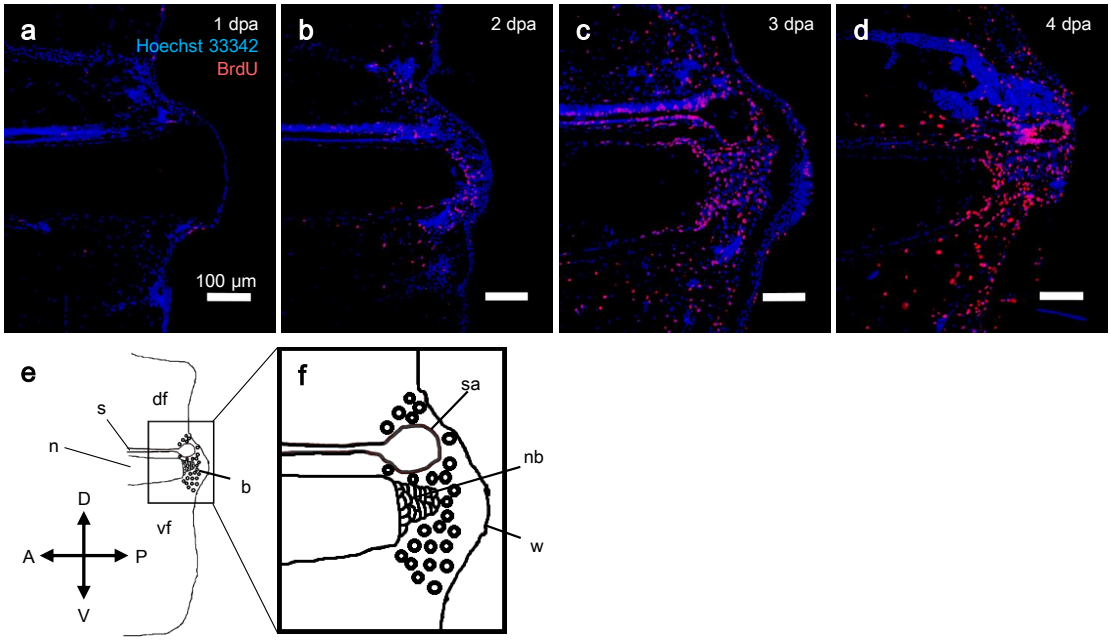

Figure 2 Proliferating cells were enriched in the tail blastema at 3 dpa

(a-d) Tail stumps of St. 49-53 tadpoles were fixed at 1, 2, 3, and 4 dpa after BrdU labelling for 12 hours, sagittal sections of them were subjected to immunohistochemistry using anti-BrdU antibody (red), and the nuclei were counterstained with Hoechst 33342 (blue). (e) Schematic drawing of a 3-dpa tail stump. (f) A magnified view of the region delineated by the square in panel (e). Anterior is to the left, and dorsal is up. Scale bars indicate 100 μm. df, dorsal fin; s, spinal cord; n, notochord; b, blastema; vf, ventral fin; sa, spinal cord ampulla; nb, notochord bud; w, wound epithelium.

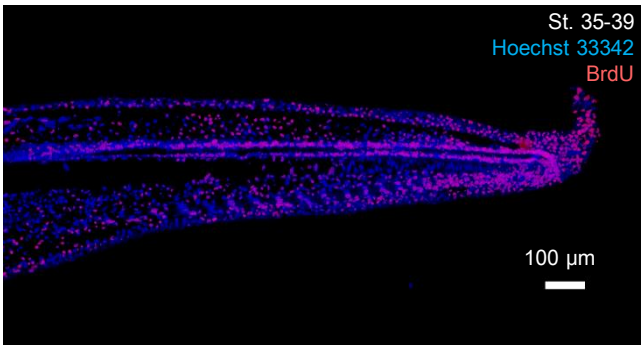

Figure 3 Proliferating cells are enriched in tailbud

Sagittal sections from tailbud of St. 35-39 tadpole which were labelled with BrdU for 12 hours before fixation were subjected to immunohistochemistry using anti-BrdU antibody (red), and the nuclei were counterstained with Hoechst 33342 (blue). Anterior is to the left, and dorsal is up. A scale bar indicates 100 μm.

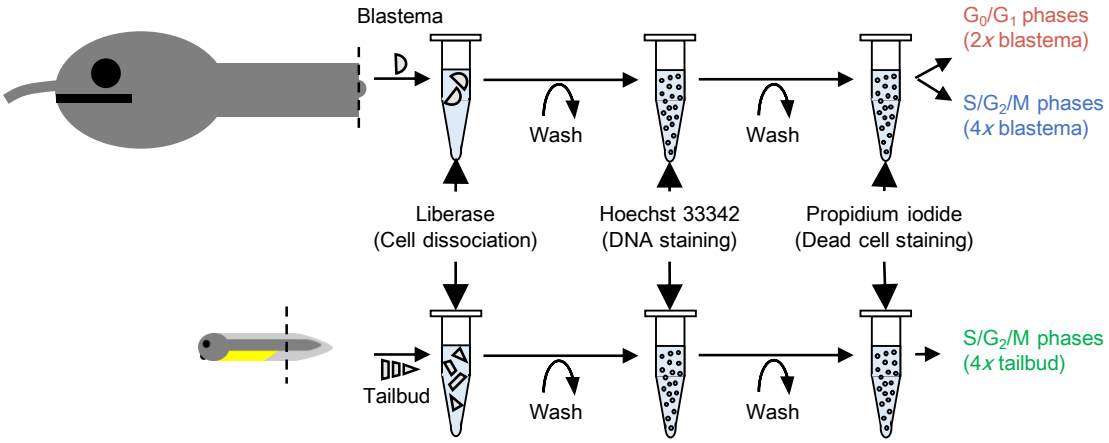

Figure 4 Cell preparation procedure for isolation of proliferating and non-proliferating tail blastema cells and proliferating tailbud cells using flow cytometry

Tailbuds of the tailbud stage embryos were amputated near the proctodeum.

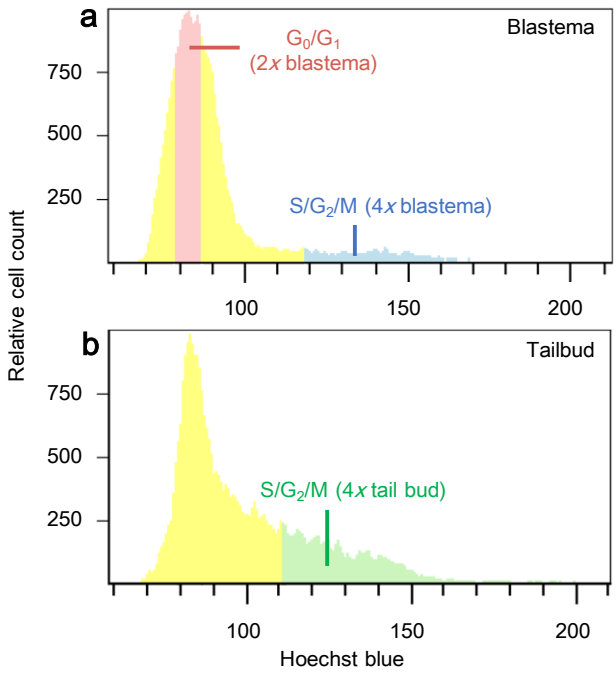

Figure 5 Cell cycle analysis using flow cytometry

Cells in tail blastemas (a) and tailbuds (b) were analysed. Horizontal axes represent fluorescent intensity of Hoechst blue, which reflects DNA contents, and vertical axes represent relative cell counts. The cells were classified into G_0/G_1 phases (major peaks), and $S/G_2/M$ phases (whose DNA contents were higher than those of cells in the major peak and lower than twice of those of cells in the major peak) based on the DNA content. Cell fractions coloured in red (‘2*x*-tail blastema’ cell fraction), blue (‘4*x*-tail blastema’ cell fraction), and green (‘4*x*-tailbud’ cell fraction), respectively, were collected and subjected to RNA-seq analysis.

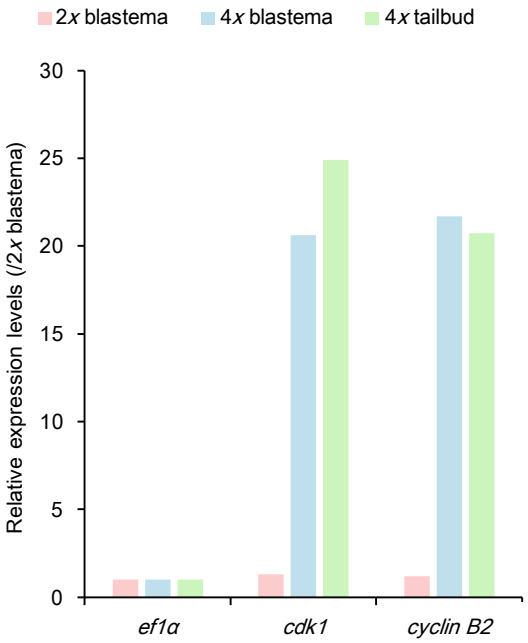

Figure 6 Comparison of expression levels of cell cycle markers

Relative expression levels were estimated from RNA-seq data, taking the values in the '2*x*-tail blastema' cell fraction as 1. Expression levels of *ef1α*, a housekeeping gene, were almost the same in all samples.

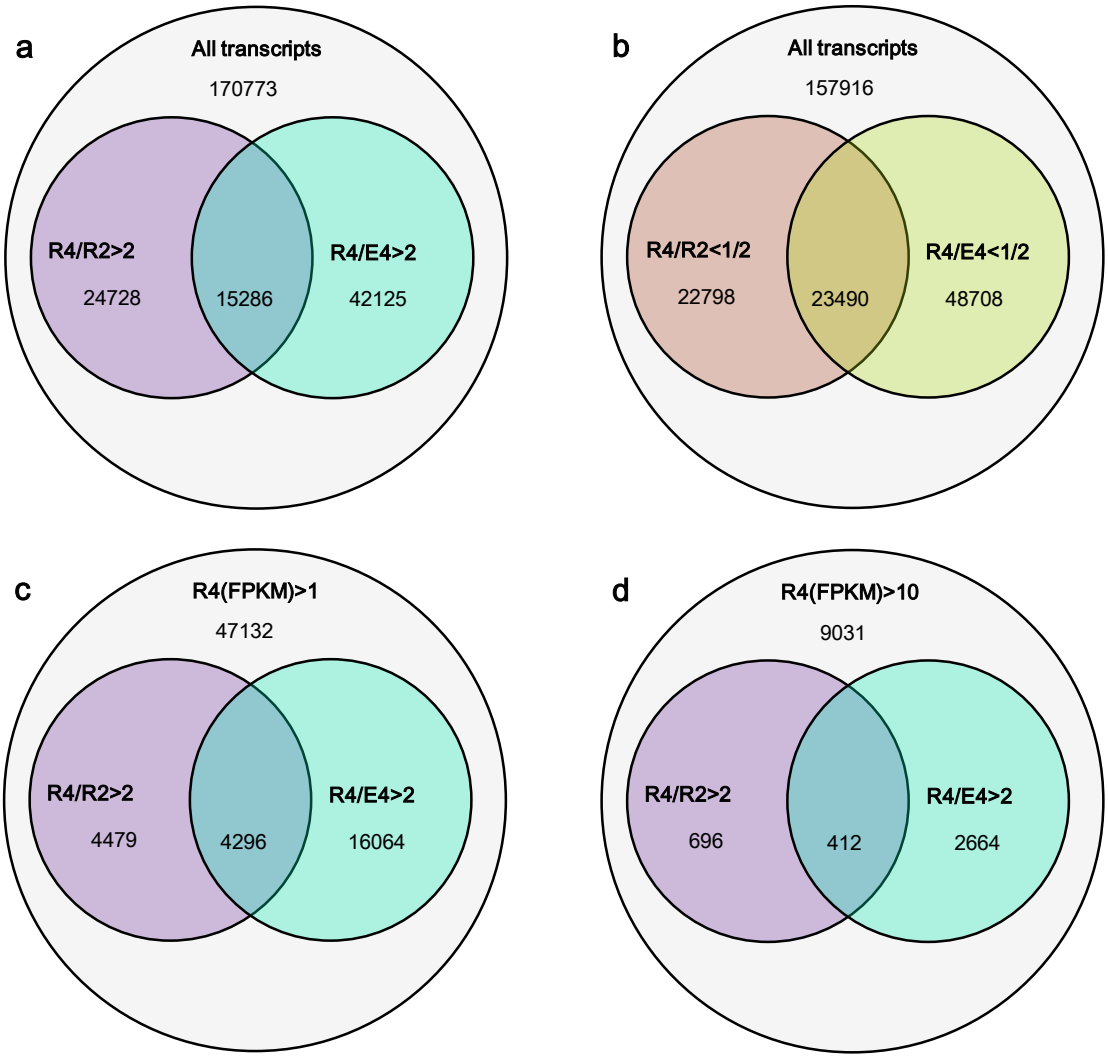

e

R4(FPKM)>10, R4/R2>2, R4/E4>2
412

↓

Maximum depth of uniquely mapped reads was at least 50
70

↓

Manually edited
41

↓

Removed ribosomal RNA
36

↓

Performed qRT-PCR
28

↓

Blastema-selective expression
10

Figure 7 RNA-seq analysis of genes preferentially expressed in proliferating or non-proliferating tail blastema cells as well as proliferating tailbud cells

Genes preferentially expressed in each cell fraction were identified by RNA-seq analysis. (a) Genes that are upregulated more than 2-folds in R4 than in R2 or E4. (b) Genes downregulated more than 2-folds in R4 than in R2 or E4. (c, d) Genes whose FPKMs in R4 were larger than 1 (c) or 10 (d). Because transcripts on the unassembled short scaffolds were also counted, the total number of genes were very high. (e) Flow chart for identification of genes expressed preferentially in the proliferating tail blastema cells.

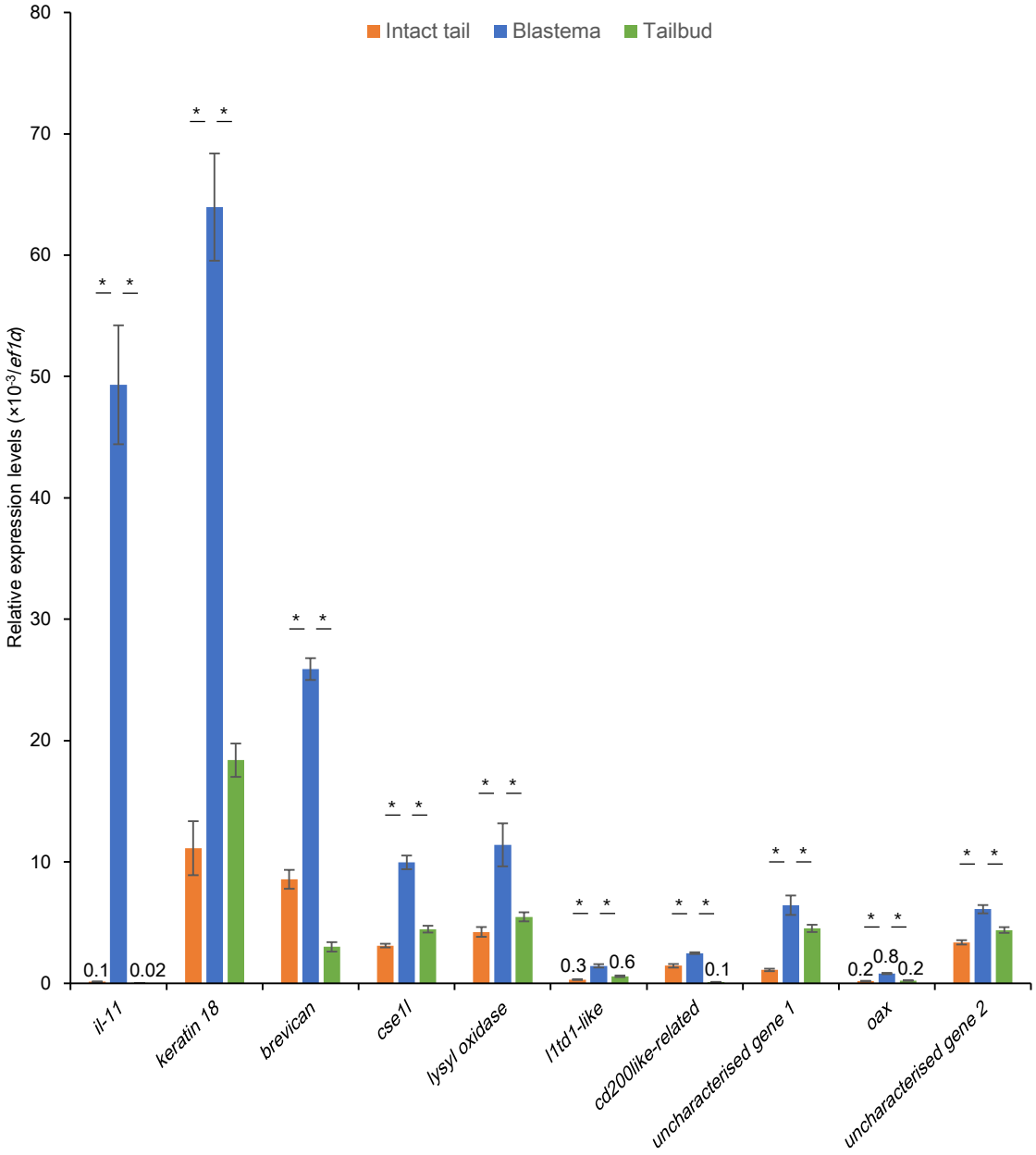

Figure 8 Identification of genes expressed preferentially in the tail blastema by qRT-PCR

The relative expression levels of the 10 genes that show the blastema-selective expression by qRT-PCR using RNAs extracted from intact tails (orange), regenerating tails (blue), and tailbuds (green). Total RNA prepared from the distal half of the intact tails of St. 49-53 tadpoles (n~25), tail blastemas of the regenerating tadpoles of the same stage 3dpa (n~100), and tailbuds of St. 35-39 tadpoles (n~100) were used. The vertical axis represents relative expression levels normalised by those of *ef1α*. The

values less than 1 were labelled. (Mean ± SE, n=4) *$P < 0.05$, Dunnett's test.

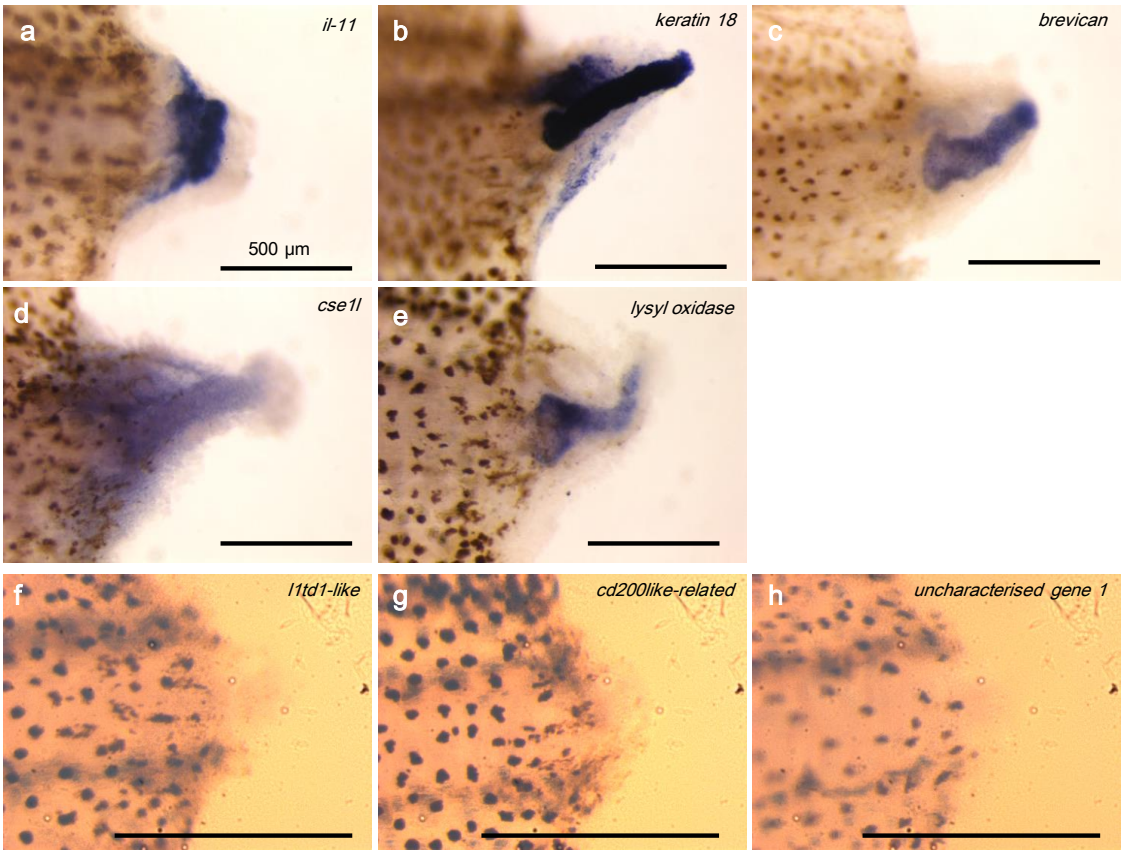

Figure 9 Candidate genes are expressed in tail blastemas

WISH of 3-dpa regenerating tails of St. 49-53 tadpoles for *il-11* (a), *keratin 18* (b), *brevican* (c), *cse1l* (d), *lysyl oxidase* (e), *l1td1-like* (f), *cd200like-related* (g), and *uncharacterised gene 1* (h) (blue/purple). Anterior is to the left, and dorsal is up. Scale bars indicate 500 µm. Brown pigments are melanophores of the tadpoles remaining after the bleaching. Note that although the morphology of the regenerating tail is slightly different, most tadpoles regenerate their tails.

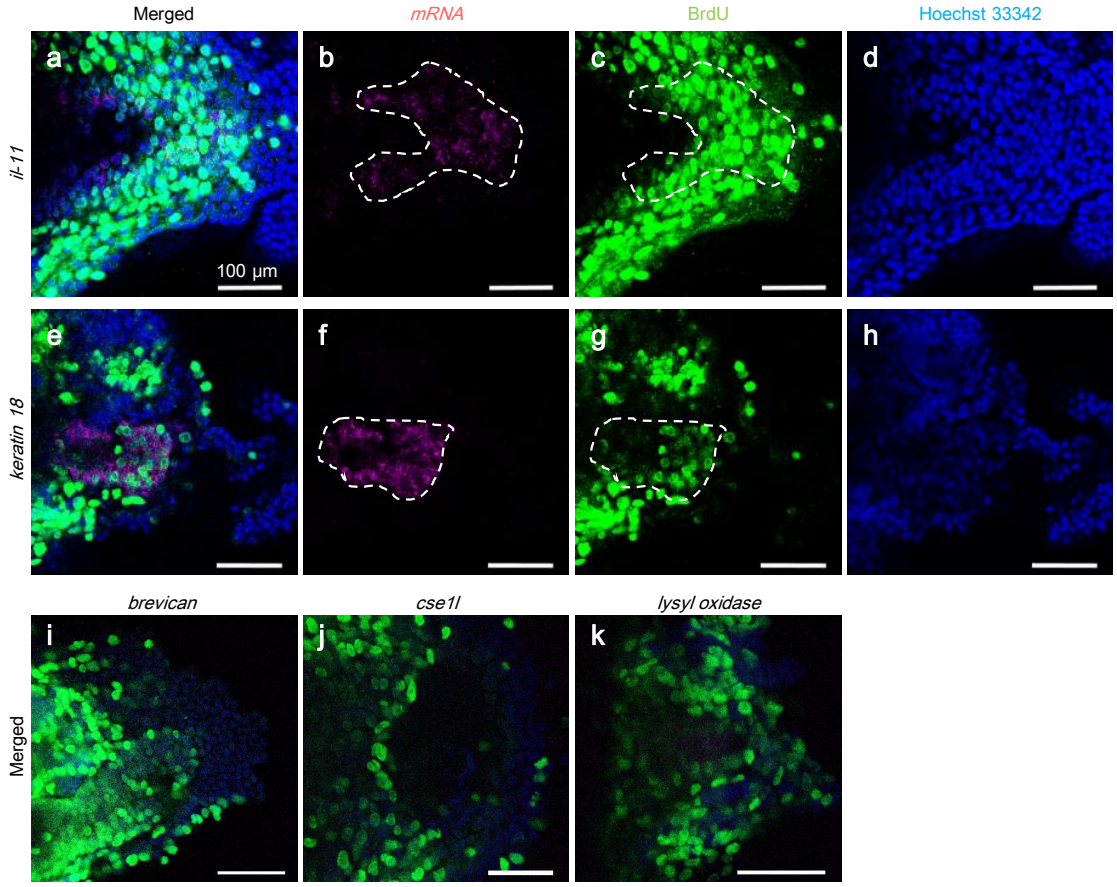

Figure 10 *il-11* and *keratin 18* are expressed in proliferating tail blastema cells

Sagittal sections of tail blastema from 3-dpa regenerating tails of St. 49-53 tadpoles were double labelled with WISH for *il-11* (a-d) *keratin 18* (e-h), *brevican* (i), *cse1l* (j), and *lysyl oxidase* (k), and 12 hour BrdU-labelling. (b) and (f) show magenta channels (mRNA), (c) and (g) show green channels (BrdU), (d) and (h) show blue channels (nuclei stained with Hoechst 33342). (a), (e), and (i-k) show merged images. Note that mRNA signals detected in the cytoplasm do not exactly merge with BrdU-signals detected in the nuclei. White broken lines indicate cell populations that highly expressed the genes. Anterior is to the left, and dorsal is up. Scale bars indicate 100 µm.

以降の内容に関しては 5 年以内に雑誌等で刊行予定のため、非公開。

Tables

Table 1. Homology search for blastema selective genes

Clone	blastn(Xenopus)	blastx(all)	blastx(-Xenopus)	Gene name
A	No hit	Turtle Interleukin 11 (XP_005312109.1)	-	*il-11*
B	*X. laevis keratin 18* (NM_001088985.1)	-	-	*keratin 18*
C	*X. laevis brevican* (NM_001088637.1)	-	-	*brevican*
D	*X. laevis cse1l* (NM_001092566.1)	-	-	*cse1l*
E	*X. laevis lysyl oxidase* (BC130090.1)	-	-	*lysyl oxidase*
F	No hit	X. tropicalis L1td1-like (XP_004917530.1)	-	*l1td1-like*
G	*X. tropicalis uncharacterized mRNA* (XM_004918270.1)	X.tropicalis Uncharacterized protein (XP_004912498.1)	Chinchilla CD200-like (XP_005386669.1)	*cd200like-related*
H	No hit	No hit	-	*uncharacterized gene 1*
I	Reverse strand of *X. laevis oax* (AF225412.1)	-	-	*oax*
J	No hit	No hit	-	*uncharacterized gene 2*

Top hits for blast search are listed. In blastn, top hits which matched query cover >0.3, and identity >0.7 are listed. blastn(Xenopus): blastn searching for Xenopus database, blastx(all): blastx searching for all non-redundant protein sequences, blastx(-Xenopus): blastx searching for all non-redundant protein sequences except Xenopus. turtle: *Chrysemys picta bellii*, chinchilla: *Chinchilla lanigera*.

以降の内容に関しては 5 年以内に雑誌等で刊行予定のため、非公開。

References

Allen, T.A., Von Kaenel, S., Goodrich, J.A., and Kugel, J.F. (2004). The SINE-encoded mouse B2 RNA represses mRNA transcription in response to heat shock. Nat. Struct. Mol. Biol. *11*, 816–821.

Altschul, S.F., Gish, W., Miller, W., Myers, E.W., and Lipman, D.J. (1990). Basic local alignment search tool. J. Mol. Biol. *215*, 403–410.

Anders, S., Pyl, P.T., and Huber, W. (2015). HTSeq-A Python framework to work with high-throughput sequencing data. Bioinformatics *31*, 166–169.

Auer, T.O., Duroure, K., De Cian, A., Concordet, J.P., and Del Bene, F. (2014). Highly efficient CRISPR/Cas9-mediated knock-in in zebrafish by homology-independent DNA repair. Genome Res. *24*, 142–153.

Bae, S., Park, J., and Kim, J.S. (2014). Cas-OFFinder: A fast and versatile algorithm that searches for potential off-target sites of Cas9 RNA-guided endonucleases. Bioinformatics *30*, 1473–1475.

Bamba, S., Andoh, A., Yasui, H., Makino, J., Kim, S., and Fujiyama, Y. (2003). Regulation of IL-11 expression in intestinal myofibroblasts: role of c-Jun AP-1- and MAPK-dependent pathways. Am. J. Physiol. Gastrointest. Liver Physiol. *285*, G529-G538.

Bartz, H., Büning-Pfaue, F., Türkel, O., and Schauer, U. (2002). Respiratory syncytial virus induces prostaglandin E2, IL-10 and IL-11 generation in antigen presenting cells. Clin. Exp. Immunol. *129*, 438–445.

Beck, C.W., Christen, B., and Slack, J.M.W. (2003). Molecular pathways needed for regeneration of spinal cord and muscle in a vertebrate. Dev. Cell *5*, 429–439.

Beck, C.W., Izpisúa Belmonte, J.C., and Christen, B. (2009). Beyond early development: Xenopus as an emerging model for the study of regenerative mechanisms. Dev. Dyn. *238*, 1226–1248.

Chang, N., Sun, C., Gao, L., Zhu, D., Xu, X., Zhu, X., Xiong, J.W., and Xi, J.J. (2013). Genome editing with RNA-guided Cas9 nuclease in zebrafish embryos. Cell Res. *23*, 465–472.

Chen, Z., Chen, D.X., Kai, Y., Khatri, I., Lamptey, B., and Gorczynski, R.M. (2008). Identification of an expressed truncated form of CD200, CD200tr, which is a physiologic antagonist of CD200-induced suppression. Transplantation *86*, 1116–1124.

Corcoran, J.P., and Ferretti, P. (1997). Keratin 8 and 18 expression in mesenchymal progenitor cells of regenerating limbs is associated with cell proliferation and differentiation. Dev. Dyn. *210*, 355–370.

Von Dassow, G., Schmidt, J.E., and Kimelman, D. (1993). Induction of the Xenopus organizer: Expression and regulation of Xnot, a novel FGF and activin-regulated homeo box gene. Genes Dev. *7*, 355–366.

Ernst, M., and Putoczki, T.L. (2014). Molecular Pathways: IL11 as a Tumor-Promoting Cytokine-Translational Implications for Cancers. Clin. Cancer Res. *20*, 5579–5588.

Fang, Y., Gupta, V., Karra, R., Holdway, J.E., Kikuchi, K., and Poss, K.D. (2013). Translational profiling of cardiomyocytes identifies an early Jak1/Stat3 injury response required for zebrafish heart regeneration. Proc. Natl. Acad. Sci. U. S. A. *110*, 13416–13421.

Frischknecht, R., and Seidenbecher, C.I. (2012). Brevican: A key proteoglycan in the perisynaptic extracellular matrix of the brain. Int. J. Biochem. Cell Biol. *44*, 1051–1054.

Fukazawa, T., Naora, Y., Kunieda, T., and Kubo, T. (2009). Suppression of the immune response potentiates tadpole tail regeneration during the refractory period. Development *136*, 2323–2327.

Gargioli, C., and Slack, J.M.W. (2004). Cell lineage tracing during Xenopus tail regeneration. Development *131*, 2669–2679.

Geach, T.J., and Dale, L. (2005). Members of the lysyl oxidase family are expressed during the development of the frog Xenopus laevis. Differentiation. *73*, 414–424.

Gont, L.K., Steinbeisser, H., Blumberg, B., and de Robertis, E.M. (1993). Tail formation as a continuation of gastrulation: the multiple cell populations of the Xenopus tailbud derive from the late blastopore lip. Development *119*, 991–1004.

Grow, M., Neff, A.W., Mescher, A.L., and King, M.W. (2006). Global analysis of gene expression in Xenopus hindlimbs during stage-dependent complete and incomplete regeneration. Dev. Dyn. *235*, 2667–2685.

Hama, H., Kurokawa, H., Kawano, H., Ando, R., Shimogori, T., Noda, H., Fukami, K., Sakaue-Sawano, A., and Miyawaki, A. (2011). Scale: a chemical approach for fluorescence imaging and reconstruction of transparent mouse brain. Nat. Neurosci. *14*, 1481–1488.

Hoek, R.M., Ruuls, S.R., Murphy, C.A., Wright, G.J., Goddard, R., Zurawski, S.M., Blom, B., Homola, M.E., Streit, W.J., Brown, M.H., et al. (2000). Down-regulation of the macrophage lineage through interaction with OX2 (CD200). Science *290*, 1768–1771.

Hoppler, S., and Vize, P.D. (2012). Xenopus protocols: post-genomic approaches (New York: Humana Press).

Hwang, W.Y., Fu, Y., Reyon, D., Maeder, M.L., Tsai, S.Q., Sander, J.D., Peterson, R.T., Yeh, J.R.J., and Joung, J.K. (2013). Efficient genome editing in zebrafish using a CRISPR-Cas system. Nat. Biotechnol. *31*, 227–229.

Isoe, Y., Okuyama, T., Taniguchi, Y., Kubo, T., and Takeuchi, H. (2012). P53 Mutation suppresses adult neurogenesis in medaka fish (Oryzias latipes). Biochem. Biophys. Res. Commun. *423*, 627–631.

James-Zorn, C., Ponferrada, V.G., Jarabek, C.J., Burns, K.A., Segerdell, E.J., Lee, J., Snyder, K., Bhattacharyya, B., Karpinka, J.B., Fortriede, J., et al. (2013). Xenbase: expansion and updates of the Xenopus model organism database. Nucleic Acids Res. *41*, D865-D870.

Kang, J., Hu, J., Karra, R., Dickson, A.L., Tornini, V.A., Nachtrab, G., Gemberling, M., Goldman, J.A., Black, B.L., and Poss, K.D. (2016). Modulation of tissue repair by regeneration enhancer elements. Nature *532*, 201–206.

Kernacki, K.A., Goebel, D.J., Poosch, M.S., and Hazlett, L.D. (1998). Early cytokine and chemokine gene expression during Pseudomonas aeruginosa corneal infection in mice. Infect. Immun. *66*, 376–379.

Kim, J.H., Lee, S.R., Li, L.H., Park, H.J., Park, J.H., Lee, K.Y., Kim, M.K., Shin, B.A., and Choi, S.Y. (2011). High cleavage efficiency of a 2A peptide derived from porcine teschovirus-1 in human cell lines, zebrafish and mice. PLoS One *6*, e18556.

King, M.W., Nguyen, T., Calley, J., Harty, M.W., Muzinich, M.C., Mescher, A.L., Chalfant, C., N'Cho, M., McLeaster, K., McEntire, J., et al. (2003). Identification of genes expressed during Xenopus laevis limb regeneration by using subtractive hybridization. Dev. Dyn. *226*, 398–409.

Kiya, T., Kunieda, T., and Kubo, T. (2008). Inducible- and constitutive-type transcript variants of. Insect Mol. Biol. *17*, 531–536.

Knapp, D., Schulz, H., Rascon, C.A., Volkmer, M., Scholz, J., Nacu, E., Le, M., Novozhilov, S., Tazaki, A., Protze, S., et al. (2013). Comparative transcriptional profiling of the axolotl limb identifies a tripartite regeneration-specific gene program. PLoS One *8*, e61352.

Kragl, M., Knapp, D., Nacu, E., Khattak, S., Maden, M., Epperlein, H.H., and Tanaka, E.M. (2009). Cells keep a memory of their tissue origin during axolotl limb regeneration. Nature *460*, 60–65.

Langmead, B., Trapnell, C., Pop, M., and Salzberg, S.L. (2009). Ultrafast and memory-efficient alignment of short DNA sequences to the human genome. Genome Biol. *10*, R25.

Lattin, J.E., Schroder, K., Su, A.I., Walker, J.R., Zhang, J., Wiltshire, T., Saijo, K., Glass, C.K., Hume, D.A., Kellie, S., et al. (2008). Expression analysis of G Protein-Coupled Receptors in mouse macrophages. Immunome Res. *4*, 5.

Lin, K.K., and Goodell, M.A. (2006). Purification of hematopoietic stem cells using the side population. Methods Enzymol. *420*, 255–264.

Lin, G., Chen, Y., and Slack, J.M.W. (2013). Imparting regenerative capacity to limbs by progenitor cell transplantation. Dev. Cell *24*, 41–51.

Liu, S.Y., Selck, C., Friedrich, B., Lutz, R., Vila-Farré, M., Dahl, A., Brandl, H., Lakshmanaperumal, N., Henry, I., and Rink, J.C. (2013). Reactivating head regrowth in a regeneration-deficient planarian species. Nature *500*, 81–84.

Love, M.I., Huber, W., and Anders, S. (2014). Moderated estimation of fold change and dispersion for RNA-seq data with DESeq2. Genome Biol. *15*, 550.

Love, N.R., Chen, Y., Bonev, B., Gilchrist, M.J., Fairclough, L., Lea, R., Mohun, T.J., Paredes, R., Zeef, L.A.H., and Amaya, E. (2011). Genome-wide analysis of gene expression during Xenopus tropicalis tadpole tail regeneration. BMC Dev. Biol. *11*, 70.

Love, N.R., Chen, Y., Ishibashi, S., Kritsiligkou, P., Lea, R., Koh, Y., Gallop, J.L., Dorey, K., and Amaya, E. (2013). Amputation-induced reactive oxygen species are required for successful Xenopus tadpole tail regeneration. Nat. Cell Biol. *15*, 222–228.

Matadeen, R., Hon, W.C., Heath, J.K., Jones, E.Y., and Fuller, S. (2007). The Dynamics of Signal Triggering in a gp130-Receptor Complex. Structure *15*, 441–448.

McGowan, C.H., Russell, P., and Reed, S.I. (1990). Periodic biosynthesis of the human M-phase promoting factor catalytic subunit p34 during the cell cycle. Mol. Cell. Biol. *10*, 3847–3851.

Miyajima, A., Tanaka, M., and Itoh, T. (2014). Stem/Progenitor Cells in Liver Development, Homeostasis, Regeneration, and Reprogramming. Cell Stem Cell *14*, 561–574.

Monaghan, J.R., Epp, L.G., Putta, S., Page, R.B., Walker, J.A., Beachy, C.K., Zhu, W., Pao, G.M., Verma, I.M., Hunter, T., et al. (2009). Microarray and cDNA sequence analysis of transcription during nerve-dependent limb regeneration. BMC Biol. *7*, 1.

Naora, Y., Hishida, Y., Fukazawa, T., Kunieda, T., and Kubo, T. (2013). Expression analysis of XPhyH-like during development and tail regeneration in Xenopus tadpoles: possible role of XPhyH-like expressing immune cells in impaired tail regenerative ability. Biochem. Biophys. Res. Commun. *431*, 152–157.

Närvä, E., Rahkonen, N., Emani, M.R., Lund, R., Pursiheimo, J.P., Nästi, J., Autio, R., Rasool, O., Denessiouk, K., Lähdesmäki, H., et al. (2012). RNA-binding protein L1TD1 interacts with LIN28 via RNA and is required for human embryonic stem cell self-renewal and cancer cell proliferation. Stem Cells *30*, 452–460.

Nieuwkoop, P.D., and Faber, J. (1994). Normal table of Xenopus laevis (Daudin). A systematical and chronological survey of the development from the fertilized egg till the end of metamorphosis. (New York: Garland Science).

Nishioka, T., Eustace, A., and West, C. (2012). Lysyl oxidase: from basic science to future cancer treatment. Cell Struct. Funct. *37*, 75–80.

Ogawa, R., Ma, Y., Yamaguchi, M., Ito, T., Watanabe, Y., Ohtani, T., Murakami, S., Uchida, S., De Gaspari, P., Uezumi, A., et al. (2015). Doublecortin marks a new population of transiently amplifying muscle progenitor cells and is required for myofiber maturation during skeletal muscle regeneration. Development *142*, 51–61.

Ogryzko, V. V, Brinkmann, E., Howard, B.H., Pastan, I., and Brinkmann, U. (1997). Antisense inhibition of CAS, the human homologue of the yeast chromosome segregation gene CSE1, interferes with mitosis in HeLa cells. Biochemistry *36*, 9493–9500.

Okada, N. (1991). SINEs. Curr. Opin. Genet. Dev. *1*, 498–504.

Pallafacchina, G., François, S., Regnault, B., Czarny, B., Dive, V., Cumano, A., Montarras, D., and Buckingham, M. (2010). An adult tissue-specific stem cell in its niche: A gene profiling analysis of in vivo quiescent and activated muscle satellite cells. Stem Cell Res. *4*, 77–91.

Park, B.Y., Hong, C.S., Weaver, J.R., Rosocha, E.M., and Saint-Jeannet, J.P. (2012). Xaml1/Runx1 is required for the specification of Rohon-Beard sensory neurons in Xenopus. Dev. Biol. *362*, 65–75.

Pearl, E.J., Barker, D., Day, R.C., and Beck, C.W. (2008). Identification of genes associated with regenerative success of Xenopus laevis hindlimbs. BMC Dev. Biol. *8*, 66.

Peterson, H., Abu Dawud, R., Garg, A., Wang, Y., Vilo, J., Xenarios, I., and Adjaye, J. (2013). Qualitative modeling identifies IL-11 as a novel regulator in maintaining self-renewal in human pluripotent stem cells. Front. Physiol. *4*, 303.

Des Portes, V., Pinard, J.M., Billuart, P., Vinet, M.C., Koulakoff, A., Carrié, A., Gelot, A., Dupuis, E., Motte, J., Berwald-Netter, Y., et al. (1998). A novel CNS gene required for neuronal migration and involved in X- linked subcortical laminar heterotopia and lissencephaly syndrome. Cell *92*, 51–61.

Robb, L., Li, R., Hartley, L., Nandurkar, H.H., Koentgen, F., and Begley, C.G. (1998). Infertility in female mice lacking the receptor for interleukin 11 is due to a defective uterine response to implantation. Nat. Med. *4*, 303–308.

Sander, V., Müllegger, J., and Lepperdinger, G. (2001). Xenopus brevican is expressed in the notochord and the brain during early embryogenesis. Mech. Dev. *102*, 251–253.

Session, A.M., Uno, Y., Kwon, T., Chapman, J.A., Toyoda, A., Takahashi, S., Fukui, A., Hikosaka, A., Suzuki, A., Kondo, M., et al. (2016). Genome evolution in the allotetraploid frog Xenopus laevis. Nature *538*, 336–343.

Sikes, J.M., and Newmark, P.A. (2013). Restoration of anterior regeneration in a planarian with limited regenerative ability. Nature *500*, 77–80.

Smith, A.G., Heath, J.K., Donaldson, D.D., Wong, G.G., Moreau, J., Stahl, M., and Rogers, D. (1988). Inhibition of pluripotential embryonic stem cell differentiation by purified polypeptides. Nature *336*, 688–690.

Stoick-Cooper, C.L., Moon, R.T., and Weidinger, G. (2007). Advances in signaling in vertebrate regeneration as a prelude to regenerative medicine. Genes Dev. *21*, 1292–1315.

Tazaki, A., Kitayama, A., Terasaka, C., Watanabe, K., Ueno, N., and Mochii, M. (2005). Macroarray-based analysis of tail regeneration in Xenopus laevis larvae. Dev. Dyn. *233*, 1394–1404.

Teramura, M., Kobayashi, S., Hoshino, S., Oshimi, K., and Mizoguchi, H. (1992). Interleukin-11 enhances human megakaryocytopoiesis in vitro. Blood *79*, 327–331.

Tober, J., Maijenburg, M.W., and Speck, N.A. (2016). Taking the Leap: Runx1 in the Formation of Blood from Endothelium. Curr. Top. Dev. Biol. *118*, 113–162.

Trapnell, C., Roberts, A., Goff, L., Pertea, G., Kim, D., Kelley, D.R., Pimentel, H., Salzberg, S.L., Rinn, J.L., and Pachter, L. (2012). Differential gene and transcript expression analysis of RNA-seq experiments with TopHat and Cufflinks. Nat. Protoc. *7*, 562–578.

Trepicchio, W.L., Bozza, M., Pedneault, G., and Dorner, A.J. (1996). Recombinant human IL-11 attenuates the inflammatory response through down-regulation of proinflammatory cytokine release and nitric oxide production. J. Immunol. *157*, 3627–3634.

Tsujioka, H., Kunieda, T., Katou, Y., Shirahige, K., and Kubo, T. (2015). Unique Gene Expression Profile of the Proliferating Xenopus Tadpole Tail Blastema Cells Deciphered by RNA-Sequencing Analysis. PLoS One *10*, e0111655.

Umesono, Y., Tasaki, J., Nishimura, Y., Hrouda, M., Kawaguchi, E., Yazawa, S., Nishimura, O., Hosoda, K., Inoue, T., and Agata, K. (2013). The molecular logic for planarian regeneration along the anterior-posterior axis. Nature *500*, 73–76.

Wakefield, L., Ackerman, E., and Gurdon, J.B. (1983). The activation of RNA synthesis by somatic nuclei injected into amphibian oocytes. Dev. Biol. *95*, 468–475.

Wasner, M., Haugwitz, U., Reinhard, W., Tschöp, K., Spiesbach, K., Lorenz, J., Mössner, J., and Engeland, K. (2003). Three CCAAT-boxes and a single cell cycle genes homology region (CHR) are the major regulating sites for transcription from the human cyclin B2 promoter. Gene *312*, 225–237.

Wellmann, A., Krenacs, L., Fest, T., Scherf, U., Pastan, I., Raffeld, M., and Brinkmann, U. (1997). Localization of the cell proliferation and apoptosis-associated CAS protein in lymphoid neoplasms. Am. J. Pathol. *150*, 25–30.

Whitehead, G.G., Makino, S., Lien, C.L., and Keating, M.T. (2005). Fgf20 Is Essential for Initiating Zebrafish Fin Regeneration. Science *310*, 1957–1960.

Wickham, H. (2009). ggplot2: Elegant Graphics for Data Analysis (Springer-Verlag New York).

Williams, R.L., Hilton, D.J., Pease, S., Willson, T.A., Stewart, C.L., Gearing, D.P., Wagner, E.F., Metcalf, D., Nicola, N.A., and Gough, N.M. (1988). Myeloid leukaemia inhibitory factor maintains the developmental potential of embryonic stem cells. Nature *336*, 684–687.

Wu, C., Orozco, C., Boyer, J., Leglise, M., Goodale, J., Batalov, S., Hodge, C.L., Haase, J., Janes, J., Huss, J.W. 3rd, et al. (2009). BioGPS: an extensible and customizable portal for querying and organizing gene annotation resources. Genome Biol. *10*, R130.

Wu, C., MacLeod, I., and Su, A.I. (2013a). BioGPS and MyGene.info: Organizing online, gene-centric information. Nucleic Acids Res. *41*, 561–565.

Wu, C., Jin, X., Tsueng, G., Afrasiabi, C., and Su, A.I. (2016). BioGPS: Building your own mash-up of gene annotations and expression profiles. Nucleic Acids Res. *44*, D313–D316.

Wu, C.H., Tsai, M.H., Ho, C.C., Chen, C.Y., and Lee, H.S. (2013b). De novo transcriptome sequencing of axolotl blastema for identification of differentially expressed genes during limb regeneration. BMC Genomics *14*, 434.

Yin, T., Taga, T., Tsang, M.L.S., Yasukawa, K., Kishimoto, T., and Yang, Y.C. (1993). Involvement of IL-6 signal transducer gp130 in IL-11-mediated signal transduction. J. Immunol. 151, 2555–2561.

Acknowledgements

I would like to express my greatest gratitude to Prof. Takeo Kubo for providing me a wonderful environment for these studies of vertebrate organ regeneration.

I would like to greatly thank Dr. Takekazu Kunieda and Dr. Taro Fukazawa for their advice for my study.

I would like to deeply thank Prof. Masanori Taira for critical reading of the doctoral thesis.

I sincerely appreciate my corroborators, Prof. Katsuhiko Shirahige and Dr. Yuki Katou, for their excellent cooperation in RNA-seq analyses. I really appreciate Ms. Yumiko Ishii for her kind assistance with FACS analysis.

Lastly, I would like to express my endless gratitude to my family and friends for their support.